Proceedings of the International Association for Shell and Spatial Structures (IASS) Symposium 2009, Valencia
Evolution and Trends in Design, Analysis and Construction of Shell and Spatial Structures
28 September – 2 October 2009, Universidad Politecnica de Valencia, Spain
Alberto DOMINGO and Carlos LAZARO (eds.)

The effect of non-Gaussian local wind loads on structural responses of long-span domed roofs

Ying SUN *, Zheng-Gang CAO, Yue WU
* School of Civil Engineering, Harbin Institute of Technology, Harbin 150090, China
sunnyhit@hit.edu.cn

Abstract

Wind tunnel experiments for several domed roofs were carried out in the boundary layer wind tunnel at Tongji University. Experimental research in this paper shows that the non-Gaussian feature of wind pressures exists in the front and wake flow area. In order to study the effect of non-Gaussian feature of wind loading on structural responses, nodal displacements, element stresses and reaction forces under wind loads with and without the consideration of non-Gaussian nature are compared. The multiple variables wind pressure field with Gaussian nature were simulated bases upon the spectral representation method by superposition waves with target spectrum feature and spatial correlation from wind tunnel tests. It is shown that the local non-Gaussian feature of wind pressure fluctuations will produce influence on the structural response of elements and nodal displacements near non-Gaussian regions under the influence of vortices.

Keywords: non-Gaussian, wind loads, long-span domed roof.

1. Introduction

Commonly used procedures in the field of wind engineering obtain loads (pressures) using aerodynamic coefficients that multiply the square of the wind velocity. Since the model representing the wind is assumed to be Gaussian and the turbulence quadratic component is neglected, the resulting wind loads are also Gaussian. This assumption has been invoked primarily for the convenience in analysis and is quite valid for loads that involve integral effects of the random pressure field over large areas due to the Central Limit Theorem. Nonetheless, experimental research has shown in recent years that the Gaussian model does not correctly describe the wind pressure field (Gi0ffre *et al.* [1], Kumar and Stathopoulos [2], Richards and Hoxey [4]). Use the Gaussian assumption to simulate pressure fluctuations from non-Gaussian zones will severely underestimate the peak suction coefficients and result in non-conservative design (Kurmar and Stathopoulos [3]). The non-Gaussian effects in pressure will result in non-Gaussian local loads, and further may give way to increased expected responses of structural elements or supporting reactions. But to what degree will this effect exist and to what case should be paid more attentions are still unknown, which will be the main purpose of this paper.

To make this clear, based on some wind tunnel tests of domed roofs, the non-Gaussian feature in some regions are identified. For implementation of comparison with results under wind pressures in Gaussian distribution, the time histories of loadings are generated in accordance with desired statistical and spectral characteristics based on spectral representation method (Shinozuka [5]). The dynamic response of a long-span rigidly jointed single-layer latticed dome is analyzed in the time domain by using the wind pressure data obtained from wind tunnel experiments and numerical simulations. The deflection of the dome and the resultant member stresses, i.e. the axial and bending stresses, are calculated at each time step. Based on the results, the different characteristics of the wind-induced dynamic response of the dome are discussed.

2. Wind tunnel test

2.1. Experiment arrangement

The wind tunnel test was conducted in the boundary layer wind tunnel TJ-2 in the school of Civil Engineering, Tongji University. The wind tunnel is of the recirculating type with a working section of 3m wide, 2.5m high and 15m long. Turbulent boundary layers were generated on the wind tunnel floor by using a set of spires together with a number of roughness blocks on the floor. The mean velocity profile and turbulence intensity profile are simulated with the target values for a suburban terrain category of $a = 0.16$, whose profile is shown in Figure 1. The reference wind tunnel speeds for the measurements were 12m/s. The pressure fluctuations were measured simultaneously by electric pressure scanners of HyScan3000 of Scanivalve Corp. The pressure signals were sampled at 312.5Hz for 19.2 seconds and were measured essentially simultaneously. Assuming that the wind tunnel/full-scale velocity ratio is 1:3, the wind velocity at the level of the eave edge is 6.7 m/s corresponding to the full scale 20m/s. Domes are designed with base diameter of 80m and rise-span-ratio of 1/6 were simulated at a scale of 1:100(Figure 2), the heights of eave varied from 15~25m. The Reynolds number based on the model base diameter and the mean wind velocity on top of model height is $4\acute{}\ 10^5$. Each time series record (0f 6000 data points) is equivalent to 10.7 minutes in full-scale.

2.2. Data processing

The wind pressure coefficients of roof surface are defined as,

$$C_{pi}(t) = \frac{P_i(t) - P_¥}{P_0 - P_¥} \tag{1}$$

where： $C_{pi}(t)$ is the pressure coefficient of tap i in the model, $P_i(t)$ is the measured pressure of tap i , P_0 , $P_¥$ is reference total pressure and reference static pressure. The reference point is at roof height. The mean and fluctuating wind pressure coefficients C_{pimean} , C_{pirms} from the $C_{pi}(t)$ time series can be calculated by means of statistical method.

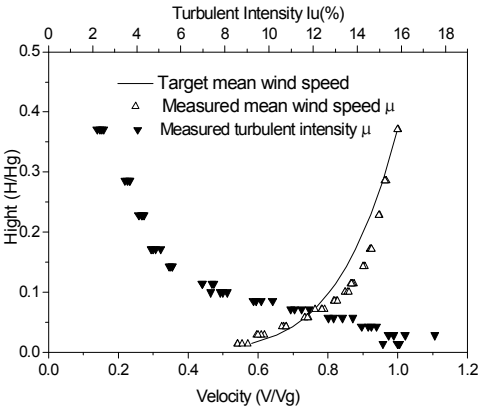

Figure 1: Wind tunnel simulation for terrain B

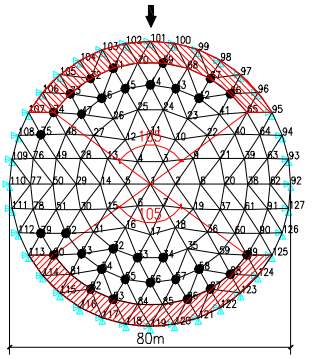

Figure 2: Wind tunnel experimental models

● the maximum nodal displacement difference between simulated and original results is bigger than 20%;

▨ non-Gaussian region.

The shape of a probability density function (PDF) of the pressure (C_p) can be characterized by its third and fourth central moments relative to the standard deviation value. The skewness coefficient C_{psk}, and the kurtosis coefficient C_{pku}, are defined, respectively, as

$$C_{pisk} = n^{-1}\sum_{i=1}^{n}[(C_{pi}(t) - C_{pimean})/C_{pirms}]^3 \quad (2)$$

$$C_{piku} = n^{-1}\sum_{i=1}^{n}\left(C_{pi}(t) - C_{pimean}\right)/C_{pirms}\right]^4 \quad (3)$$

For a normal or Gaussian distribution, skewness and kurtosis coefficients are equal to 0 and 3, respectively. Values of C_{psk} and C_{pku} different from 0 and 3 indicate that the data sets considered may not be Gaussian. C_{psk} <0 corresponds to skewness to the left, while C_{psk} >0 to the right. Large negative skewness coefficient results in probabilities for negative pressure fluctuations much higher than those for Gaussian processes. C_{pku} >3 represents distributions more peaked than the Gaussian and C_{pku} <3 characterizes distributions flatter than the Gaussian, as shown in Figure 3. The intensity and occurrence of pressure spikes are usually governed by the value assigned to the kurtosis. As illustrated above, the skewness and kurtosis coefficients can be used to describe the characteristics deviate from Gaussian features.

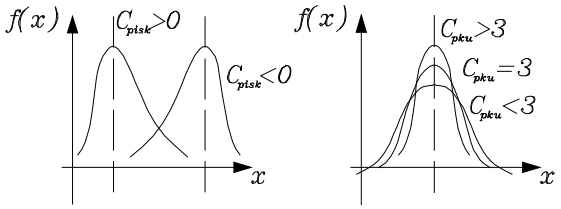

Figure 3: Statistical moments for description of non-Gaussian features

3. Numerical simulation for wind pressure field with Gaussian feature

In order to quantify the effect of non-Gaussian on the structural response, the wind pressure field in Gaussian distribution is simulated. Firstly, a procedure to produce a random Gaussian wind pressure field with target spatial-temporal characteristics (the same as wind tunnel) is introduced. Since the wind pressures vary spatially as well as in time, the time space correlation of the pressure fluctuations would play an important role in the dome's dynamic response. The difference between the simulated and original time series lies in moment statistics higher than second order, that is, skewness and kurtosis coefficients. This simulation process is carried out by using spectral representation method, the detail process is as follows.

To simulate a set of sample time series, the two-side cross-power spectral density matrix $S(w)$ is decomposed in such a way that,

$$S(w) = H(w)H^{*}(w)' \tag{4}$$

in which $S_{ij}(w)$ is the (*i*,*j*) element of $S(w)$, derived from the wind tunnel data; *H* is a (*n* × *n*) matrix; and H^{*} is the complex conjugate of *H*. For the simulation purpose, *H* is usually chosen to be a lower triangular matrix. A sample function of the dynamic wind load on the *j*th floor can be simulated following Shinozuka (Shinozuka [5]),

$$w_j(t) = \sum_{m=1}^{j}\sum_{l=1}^{N}\sqrt{Dw}\left|H_{jm}(w_i)\right|\cos\left(w_l t + q_{jm}(w_l) + f_{ml}\right) \tag{5}$$

where H_{jm} is the (*j, m*) element of the matrix *H*; *N* is the total discrete frequency points; f_{ml} are independent random numbers uniformly distributed between 0 to $2p$; $w_l = (l-1)Dw$ is the *lth* frequency with Dw being the sampling frequency; and

$$q_{jm}(w_l) = \tan^{-1}\left[\frac{\mathrm{Im}\,H_{jm}(w_l)}{\mathrm{Re}\,H_{jm}(w_l)}\right] \tag{6}$$

4. Structural analysis

The model for the analysis is a rigidly jointed single-layer latticed dome with a triangular network (see Figure 2), the division number of the network is 6, with the same point number of wind tunnel testing taps. The members are steel pipes specified in the Chinese Industrial Standard. The analysis programme chosen here is ANSYS, applying a finite element method to the latticed dome, the dynamic motion of the dome can be represented by a linear system. Use modified Newton-Raphson method for the transient analysis and assume that the damping matrix (Raleigh damping) is given by

$$[C] = a[M] + b[K] \tag{7}$$

The values of the coefficients *a* and *b* are determined such that the critical damping ratios for the first and second modes become 0.02, which is often used in the design of steel structures. Such an assumption may result in an overestimation or underestimation of the response to some degree. However, the effects have not been clarified yet in a quantitative sense.

The wind load, expressed as a concentrated load at the interior node of the network, is given by the product of the wind pressure at the location of the node and the tributary area of the node. The effect of the internal pressure is not considered here.

The dome's response is analyzed for a time duration of 10.67 min in total for each run. The result for the first 1 min is not used for the statistical analysis of the response because of the non-stationarity. In this paper, we focus on the comparisons of maximum deflection and the resultant member stresses.

5. Experiment and simulation results

5.1. The non-Gaussian nature of the wind pressure field

Until now, most researches about non-Gaussian feature of wind pressures are related to the buildings with sharp edges, very few studies concern about buildings with curve surfaces. Different with wind field above roofs with sharp edges, flow around curve surfaces don't create obvious separation vortex caused by leading edges, but it was commonly seen in previous experiments (Tamura *et al.* [7]) that horse-shoe vortex exists in front and arch-shaped vortex at the back side of dome. The wind pressures on these points under the influence of vortices have obvious deviations from a Gaussian distribution as shown in Figure 4 with the first four moment statistics and in Figure 5 from the histograms of the normalized time histories $\left(C_{pi}(t) - C_{pimean}\right)/C_{pirms}$ of the selected samples on roofs. For some typical sample time series, there are obvious sharp negative spikes intermittently displayed. The simulation results are also included in these figures.

In this study, a particular roof region is considered non-Gaussian if the absolute values of skewness and kurtosis of pressure fluctuations at various taps are greater thatn 0.2 and 3.5 respectively, detail information can refer to Sun [6], the non-Gaussian regions are shown in Figure 2 as inclined areas.

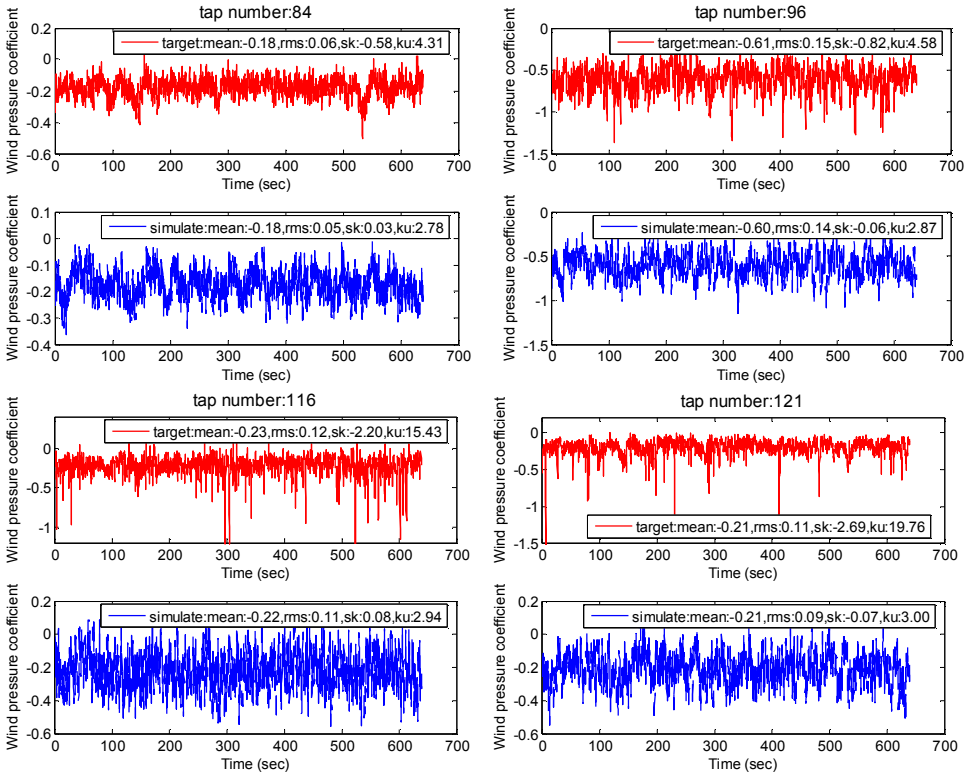

Figure 4: Wind tunnel and simulated wind pressure coefficient time series of some typical taps from which the Gaussian distribution of the signals can be recognized.

5.2. The verification of simulated wind pressures

As mentioned before, in order to study the effect of non-Gaussianity on the structural responses, another wind pressure field with Gaussian feature is simulated, with the preconditions that the power spectral density functions and temporal-spatial correlation characteristics should be the same as those of wind tunnel measurement. Figure 6 shows the comparison between experiment and simulation for the spectrum function of the pressure coefficient. As shown in the figure, the pressure fluctuations are well simulated for spectrum characteristics even in higher frequencies. The results of cross-coefficients are shown in Figure 7 (the position of taps shown in Figure 5), for taps located close to each other the correlation fit very well, but for taps far from each other the correlation of Gaussian field is higher than that of experiment data in higher frequency.

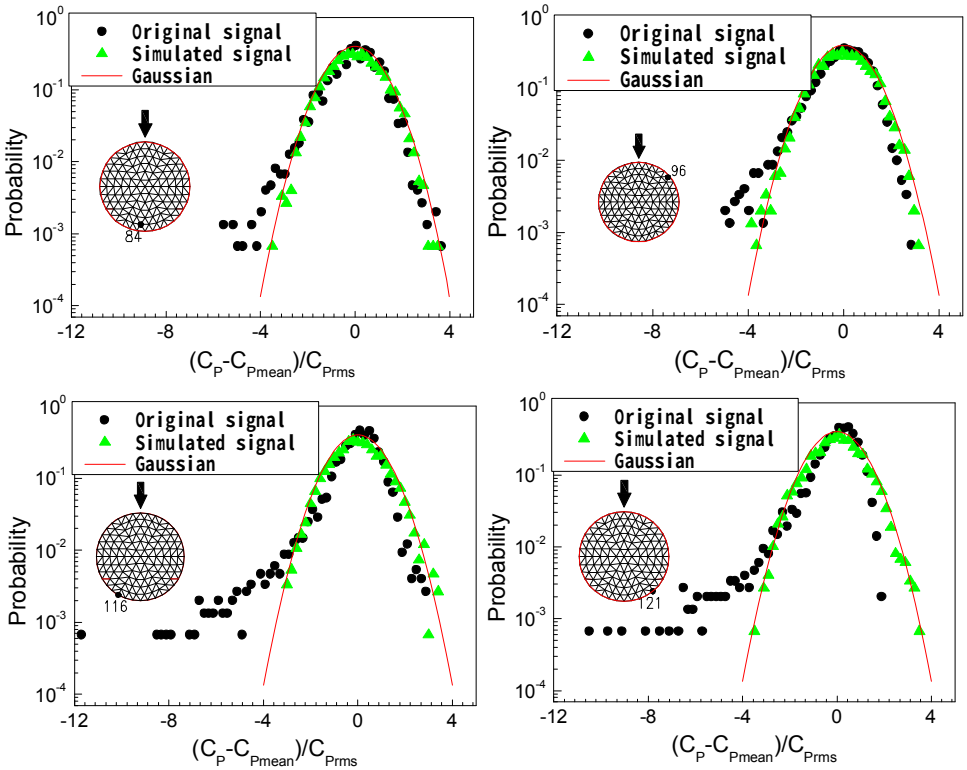

Figure 5: PDFs of some typical taps based on wind tunnel data and simulated results

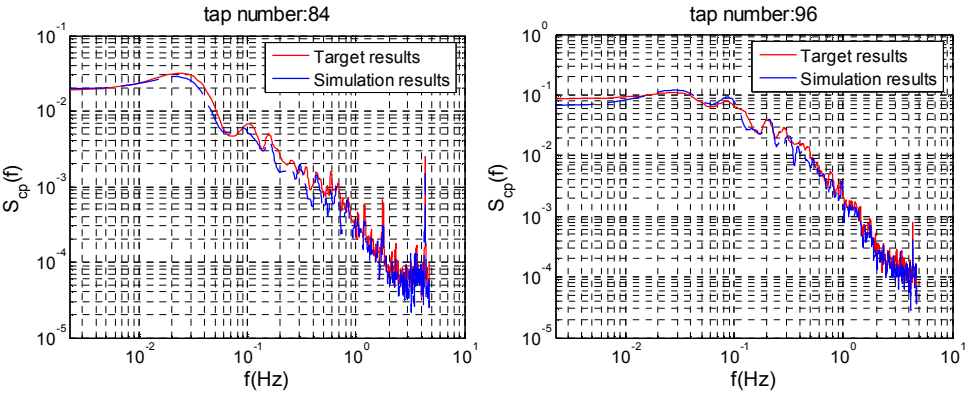

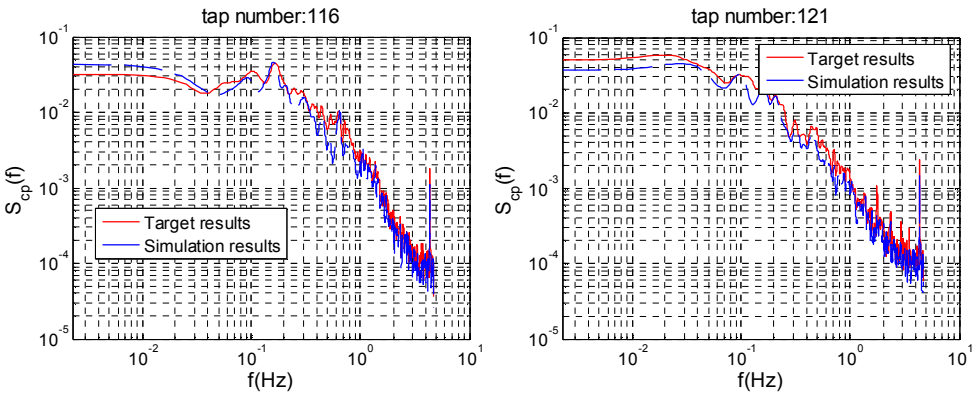

Figure 6: Spectrum functions of some typical taps based on wind tunnel data and simulated results

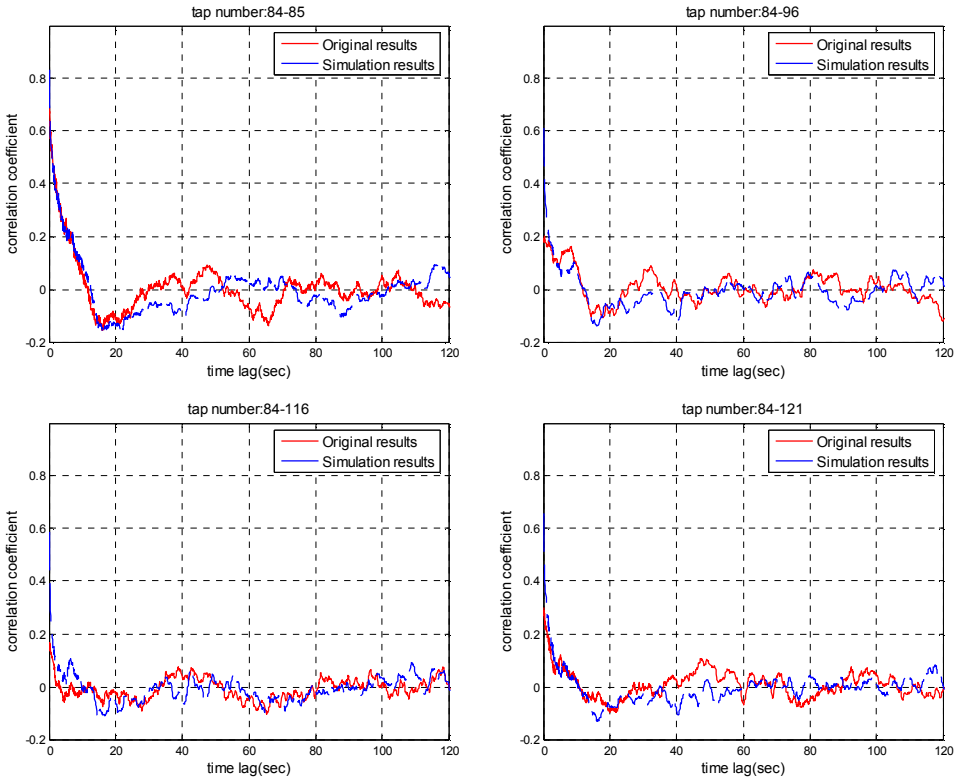

Figure 7: Comparisons of correlation coefficients

5.3. The comparison of structural responses

According to the analysis method mentioned before, the deflection of the dome, the reaction forces and the resultant member stresses, i.e. the axial and bending stresses, are recorded at each time step. In order to quantified the difference between results based on wind tunnel data and simulated data, an relative difference level coefficient *Diff* is defined as,

$$Diff = \frac{Val_{ori} - Val_{sim}}{Val_{ori}} \times 100\% \tag{8}$$

in which Val_{ori} and Val_{sim} are the results based on original experiment data and simulated data respectively. Since designers usually just care for the maximum response of structure, therefore only the maximum results are shown in the following context.

Figure 8 shows the results for sum of nodal displacements, which is the combination of X, Y and Z direction. As shown in the figure, the nodal displacement under wind tunnel data (with local non-Gaussian features) are usually larger than that of simulated results (all in Gaussian distribution), and the average difference level is 15.9%, and those nodes with difference level bigger than 20% are shown in Figure 2 with sign '●', which are located near the non-Gaussian regions.

Figure 9 gives the results of reaction forces in Z direction, in which the node number from 92 to 110 locate in the windward face, and 111 to 127 in the leeward face. It is shown that there is not big difference for the reaction forces, and even the reaction forces under simulated Gaussian field are litter bigger than that of original results, expect for that in the middle of the backward location, where the wake vortex action is strong.

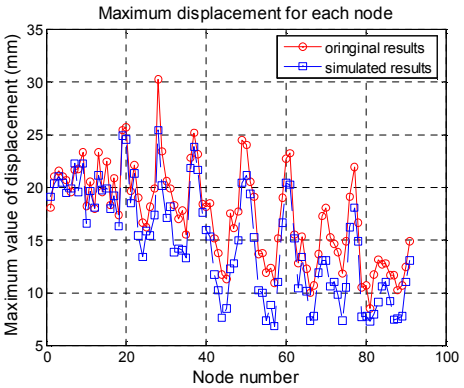

Figure 8: Maximum nodal displacements

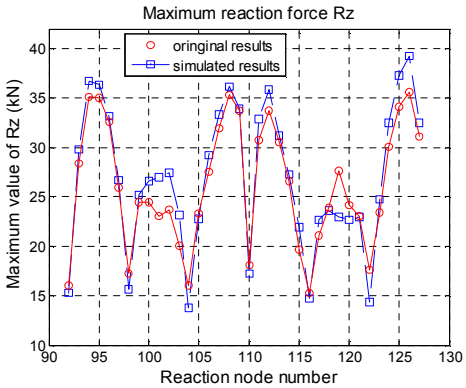

Figure 9:Maximum reaction forces in Z direction

Figure 10 shows the results of member stresses, in which the maximum stress for member section is (direct stress + bending stress) and minimum stress is (direct stress - bending stress). The average different level is 17.1%, only those results for difference level of stresses higher than 20% are plotted in the figures. And the positions for these elements are

also displayed in Figure 11, most of which also located near and in the non-Gaussian regions.

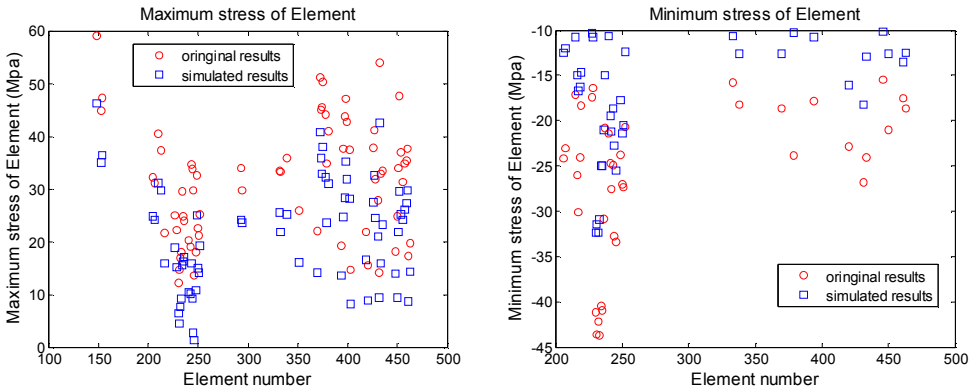

Figure 10: Maximum and Minimum stresses of elements for difference level higher than 20%

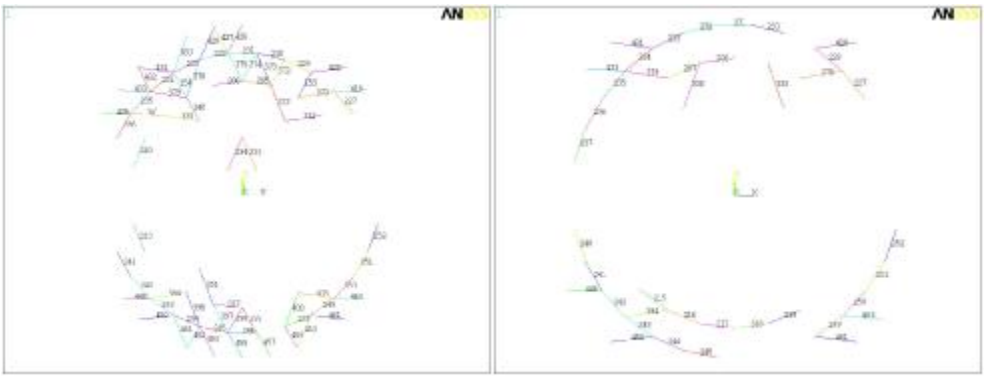

(a) Maximum stresses (b) Minimum stresses

Figure 11: Elements with difference level higher than 20% for extreme stresses of elements

6. Conclusion

This paper summarizes the non-Gaussian characteristics of measured pressure data on long span domed roofs, and studies the effect of the non-Gaussian feature on the structural responses. In order to do this, another wind pressure field with Gaussian property was simulated based on spectral representation method. The results obtained from examination reveal that wind pressure in the location of regions where the vortices such as horse-shoe vortex in front and arch-shaped vortex in the wake region take action has eminent non-Gaussian characteristics. The non-Gaussian nature of local pressure will affect some of the

structural responses around the region, especially for the displacement and element stresses, but may not cause obvious difference for reaction forces.

Acknowledgement

The supports of the National Science Foundation of China (NSFC) under project No. 90815021 and No. 50708030 are gratefully acknowledged. The assistance from Mr. Song JinZhong, Dr. Huang Peng and Dr. Zhao Lin in Tongji University with the wind tunnel experiments is gratefully acknowledged.

References

[1] Gioffre M., Gusella V. and Grigoriu M., Non-Gaussian wind pressure on prismatic buildings. II: Numerical simulation, *Journal of Structural Engineering*, (2001); 127(9); 990-995.

[2] Kumar and T. Stathopoulos, Wind loads on low building roofs: A stochastic perspective, *Journal of Structural Engineering*, 2000; 126(8); 944- 956.

[3] Kurmar K.S. and Stathopoulos T., A computerized approach replacing wind pressure time series databases, *8th ASCE Specialty conference on probabilistic mechanics and structural reliability*, PMC2000-018. 2000

[4] Richards P. J and Hoxey R. P, Quasi-steady theory and point pressures on a cubic building , *J. Wind Eng. Ind. Aerodyn.*, 2004; 92; 1173-1190.

[5] Shinozuka, M., Stochastic fields and their digital simulation, *Lecture Notes for CISM Course on Stochastic Methods in Structural Mechanics*, Hermes, Udine, Italy, 1985.

[6] Sun Y.，Wu Y.，Shen S.Z.. The non-gaussian features of wind pressure on large-span roofs[C]. *IASS-APCS 2006*, Beijing, 2006; 10; 354-355.

[7] Tamura Tetsuro, Kuwahara Kunio and Suzuki Masahiro. Numerical study of wind pressures on a Domed roof and near wake flows. *Journal of Wind Engineering and Industrial Aerodynamics*, Volume 36, Part 2, 1990, Pages 1001-1010